International Journal of Electrical and Computer Engineering (IJECE)
Vol. 16, No. 2, April 2026, pp. 753~765
ISSN: 2088-8708, DOI: 10.11591/ijece.v16i2.pp753-765

An energy-optimized A* algorithm for path planning of autonomous underwater vehicles in dynamic flow fields

Do Khac Tiep, Nguyen Van Tien, Cao Duc Thanh
Faculty of Electrical and Electronic Engineering, Vietnam Maritime University, Haiphong, Vietnam

Article Info

Article history:

Received Mar 31, 2025
Revised Dec 13, 2025
Accepted Jan 16, 2026

Keywords:

A* algorithm
Autonomous underwater vehicles
Energy-optimized
Heuristic search
Path planning

ABSTRACT

This paper presents the development and implementation of an energy-optimized A* algorithm for autonomous underwater vehicle (AUV) path planning in these complex environments. The core of the approach is the integration of a computationally efficient flow field model and a detailed AUV energy consumption model directly into the A* search heuristic. The energy model considers factors such as drag forces, relative velocity between the AUV and the flow, and AUV maneuvering. The A* cost function is modified to prioritize paths that minimize the predicted total energy expenditure, while simultaneously ensuring obstacle avoidance and path feasibility. The algorithm was implemented and validated using a simulated environment with varying flow conditions. Results demonstrate that the proposed energy-optimized A* algorithm achieves a significant reduction in energy consumption – up to 50% in tested scenarios – compared to a standard A* implementation, while successfully generating collision-free and dynamically feasible paths. This work contributes a practical and effective solution for energy-aware AUV navigation in dynamic underwater environments, enabling longer mission durations and improved operational efficiency.

Corresponding Author:

Do Khac Tiep
Electrical and Electronic Engineering, Vietnam Maritime University
484 Lach Tray, Le Chan, Hai Phong, Vietnam
Email: dokhactiep@vimaru.edu.vn

1. INTRODUCTION

Autonomous underwater vehicles (AUVs) are increasingly deployed in a wide range of applications, including oceanographic research, environmental monitoring, underwater infrastructure inspection, and military operations [1], [2]. A key challenge in AUV operations, particularly for long-duration missions, is the limited onboard energy capacity. Therefore, energy-efficient path planning is crucial for maximizing mission range, endurance, and overall effectiveness [3], [4]. This is especially true in dynamic environments characterized by strong and time-varying ocean currents, where naive path planning strategies can lead to significantly increased energy consumption and even mission failure [5], [6].

Traditional path planning algorithms, such as A*, Dijkstra's algorithm, and potential field methods, have been widely applied to AUVs [7]–[9]. However, these methods often do not explicitly account for the complex hydrodynamic forces acting on the vehicle in a dynamic flow field. Simply finding the shortest geometric path may not be energy-efficient when strong currents are present [10]. Recent research has focused on developing energy-aware path planning techniques that incorporate flow field information and vehicle dynamics [11]–[13]. These approaches often involve using computational fluid dynamics (CFD) simulations or analytical models to estimate the energy cost of traversing different paths [6], [14]. Other approaches include the use of evolutionary algorithms [15], [16] and reinforcement learning [17].

While some progress has been made, there remains a need for computationally efficient and practical path planning algorithms that can effectively minimize energy consumption in real-time or near-real-time AUV operations. Furthermore, the integration of detailed energy consumption models that account for a variety of factors (*e.g.* drag, added mass, maneuvering) is often computationally demanding and may not be suitable for resource-constrained AUV platforms [18], [19]. Some research addresses path planning in 3D environments [20]–[22], while other studies focus on multiple AUV systems [23]. There are also works focus on the uncertainty in the environment [24].

While the existing literature has made significant strides in energy-aware planning, a gap remains for a computationally efficient algorithm that seamlessly integrates a detailed energy consumption model into a classical search framework for practical, near-real-time application. Previous works often trade off model fidelity for speed or vice versa. For instance, [6] offers high accuracy but is computationally prohibitive for online use, while [15] may struggle with convergence or guarantee optimality. This paper addresses this gap by presenting a novel energy-optimized A algorithm* that is both computationally efficient and effective. Our key contributions are:

- Tight integration of models: The novel integration of a computationally efficient flow field model and a detailed AUV energy consumption model—considering drag forces, relative velocity, and maneuvering costs—directly into the A* heuristic search.
- Computational efficiency: The proposed method maintains the simplicity and guarantees of the A* algorithm while significantly improving energy economy, making it suitable for online path planning.
- Comprehensive validation: Extensive simulation across diverse scenarios (static/dynamic obstacles, weak/strong currents) demonstrates the algorithm's robustness and performance, showing up to a 50% reduction in energy consumption compared to a standard A* implementation.

The remainder of this paper is organized as follows: section 2 reviews related work on AUV path planning. Section 3 describes the proposed energy-optimized A* algorithm. Section 4 presents the simulation results and analysis. Finally, section 5 concludes the paper.

2. MODELING APPROACHES

2.1. AUV kinematics model for path planning

To accurately simulate the AUV's trajectory and estimate its position over time, we utilize two coordinate frames: an Earth-fixed frame $(O_E X_E Y_E Z_E)$ and a body-fixed frame $(OX_O Y_O Z_O)$ as shown in Figure 1. The AUV's motion is modeled using rigid-body kinematics, considering all six degrees of freedom (6DoF). These include surge, sway, and heave for translational motion, and roll, pitch, and yaw for rotational motion. Equation (1) defines these kinematic relationships.

$$\dot{p} = v = \begin{bmatrix} \dot{x} \\ \dot{y} \\ \dot{z} \end{bmatrix} = R(\phi, \theta, \psi). \begin{bmatrix} u \\ v \\ w \end{bmatrix} \tag{1}$$

where p- Position in global frame (x, y, z); v- Velocity in global frame; $R(\phi, \theta, \psi)$- Rotation matrix from body to global frame; u, v, w- Surge, sway, and heave velocities (body frame).

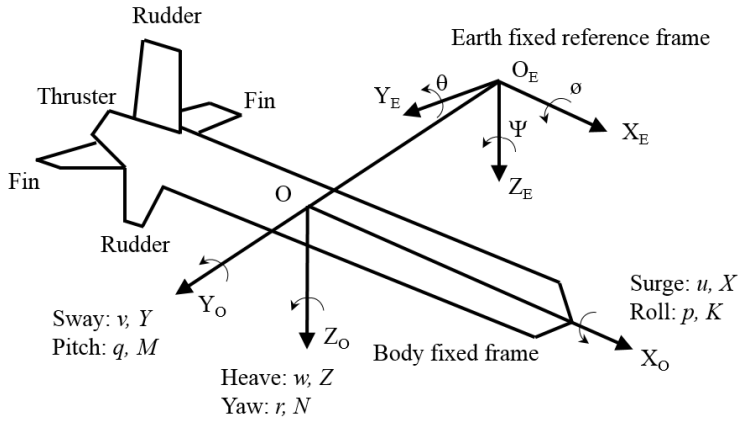

Figure 1. AUV coordinate systems

The AUV's position is updated by integrating the translational velocities over each time step as shown in (2).

$$p_{k+1} = p_k + v_k.\Delta t \quad (2)$$

Updating velocity is an important step for simulating or predicting motion. In this method, we will examine how to perform the update, with the simplifying assumption that speed is kept constant in each calculation step.

$$v_{k+1} = v_k + a_k.\Delta t \quad (3)$$

where v_{k+1} is the velocity vector at the next time step (k+1); v_k is the velocity vector at the current time step (k); a_k is the acceleration vector at the current time step (k); Δt is the time step duration. Based on the angular velocity, the change in Euler angles can be calculated as presented in (4).

$$\Theta_{k+1} = \Theta_k + \dot{\Theta}_k.\Delta t \quad (4)$$

where Θ_{k+1} is the state (likely angles, given the previous prompts about Euler angles) at the next time step (k+1); Θ_k is the state at the current time step (k); $\dot{\Theta}_k$ is the rate of change of the state (angular velocity) at the current time step (k).

The integration of the kinematic model with the energy model is crucial. Velocity serves as the link, connecting kinematic aspects with energy consumption, as indicated in (5).

$$E_{prop\infty}\|v\|^3 = (u^2 + v^2 + w^2)^{3/2} \quad (5)$$

Optimal paths balance kinematic feasibility (turn radii, acceleration) and energy efficiency.

2.2. Energy consumption model for AUV path planning

The total energy consumption (E_{Total}) of an autonomous underwater vehicle (AUV) is typically modeled by summing several core components: propulsion energy, drag loss induced by currents, and the static base load of onboard electronics.

First, propulsion energy (E_{prop}) represents the energy consumed by the propulsion system to overcome hydrodynamic drag and maintain the AUV's desired velocity (v). The power required for propulsion P_{prop} is often modeled as a function of the AUV's speed (magnitude of velocity, $\|v\|$), as indicated in (6).

$$P_{prop}(v) = k_1 v^3 + k_2 v^2 \quad (6)$$

Here, k_1 is a coefficient associated with cubic drag effects (which dominate at higher speeds), and k_2 relates to quadratic drag effects, such as skin friction. The energy consumed during a small-time step Δt at step i is calculated as (7):

$$E_{prop,i} = (k_1\|v_i\|^3 + k_2\|v_i\|^2)\Delta t \quad (7)$$

Second, we account for drag loss from currents (E_{drag}): This component accounts for the additional energy expenditure due to the presence of water currents. It depends on the relative velocity (v_{rel}) between the AUV (v_{AUV}) and the current ($v_{current}$), defined as: $v_{rel} = v_{AUV} - v_{current}$.
The energy associated with this effect over a time step Δt at step i is modeled as (8).

$$E_{drag,i} = k_3\left\|v_{rel,i}\right\|^2.\Delta t \quad (8)$$

where k_3 is a modeling coefficient. This term specifically represents the energy wasted or additionally consumed when the AUV is operating against or across currents.

Finally, static energy (E_{static}) accounts for the constant power draw (p_{static}) of sensors, navigation systems, and control hardware, which remains active regardless of motion. Over the total mission duration t, this base load is calculated as (9):

$$E_{static} = P_{static}.T_{Total} \quad (9)$$

where P_{static} represents the constant static power draw.

The total energy consumption, E_{total}, is determined by summing the propulsion energy (E_{prop}) and the drag loss from currents (E_{drag}) over all time steps, and adding the total static energy (E_{static}) as (10).

$$E_{Total} = E_{prop,i} + E_{drag,i} + E_{static} \quad (10)$$

In addition to other factors, elements such as hydrodynamic modeling, current effects, and battery efficiency also significantly influence the energy consumption of AUVs.

3. PROPOSED A* ALGORITHM

3.1. A* algorithm overview

The A* (A-star) algorithm is a powerful, informed search algorithm used to find the optimal path between a start and goal node in a graph. Unlike uninformed searches like Breadth-first search, A* employs a heuristic function, *h(n)*, to estimate the remaining cost from a node *n* to the goal. This heuristic guides the search, prioritizing nodes that appear closer to the solution.

A* combines aspects of Dijkstra's algorithm (which considers the cost-so-far) and Greedy best-first search (which relies solely on the heuristic). It achieves this by using an evaluation function, $f(n)$, for each node n:

$$f(n) = g(n) + h(n) \quad (11)$$

where $g(n)$ is the actual cost of the path from the start node to node n; $h(n)$ is the estimated cost from node n to the goal (the heuristic).

The A* algorithm efficiently finds the shortest path by maintaining an OPEN list (priority queue) of nodes to explore and a CLOSED list of processed nodes. It iteratively selects the node with the lowest estimated total cost ($f(n) = g(n) + h(n)$), expanding its neighbors and updating costs if a better path is found. The algorithm terminates when the goal is reached, reconstructing the path via parent pointers, or when the OPEN list is empty, indicating no solution. The performance relies heavily on an admissible and consistent heuristic function, ensuring optimality and completeness.

3.2. Energy-optimized A* algorithm for AUV path planning

The core challenge of path planning for AUVs in dynamic environments extends beyond merely finding a collision-free geometric path. The primary objective is to compute a trajectory that is both feasible and energy-optimal, accounting for the complex interplay between the vehicle's kinematics and the surrounding hydrodynamic forces exerted by ocean currents. Traditional shortest-path planners fail to address this objective, as they do not consider the significant energy cost of moving against or across strong flows. To address this limitation, we formulate the AUV path planning problem as a constrained optimization over the space of feasible trajectories. The objective is to minimize the total propulsive energy consumption, derived from a detailed vehicle dynamics and energy model, while adhering to constraints including obstacle avoidance, vehicle kinematic constraints, and the dynamic flow field.

Our approach builds upon the classic A* algorithm due to its optimality and completeness guarantees. The key innovation lies in the novel integration of a physics-based energy consumption model directly into the algorithm's core cost function. This transforms the search objective from minimizing geometric distance to minimizing predicted energy expenditure. The high-level architecture of our proposed method is illustrated in Figure 2, which outlines the main data flow and computational modules.

The proposed system architecture for energy-optimized path planning comprises three main components: input, processing, and output. The input module integrates the start/goal positions, obstacle map, flow field data, and AUV model parameters including dynamics and drag coefficients. Central to the processing module is the energy-optimized A* algorithm, which incorporates a specialized energy consumption model and cost function $f(n) = g_{energy}(n) + h(n)$ to evaluate paths based on energy expenditure rather than mere distance. The output generates an energy-optimal path alongside its total energy consumption estimate, completing an integrated planning framework that explicitly considers hydrodynamic influences on AUV navigation efficiency.

We formulate the AUV path planning problem as a constrained optimization over the space of feasible trajectories, with the objective of minimizing total energy consumption while respecting dynamic and environmental constraints. In planning algorithms like A*, each node in the search space is precisely a point in the AUV's state space. Defining this state space is the first step in modeling the problem. Let the AUV state at time step *i* be defined as: $s_i = (p_i, v_i, t_i)$. Where $p_i \in R^3$is position (*x, y, depth*); $v_i \in R^3$ is velocity vector; t_i is time stamp.

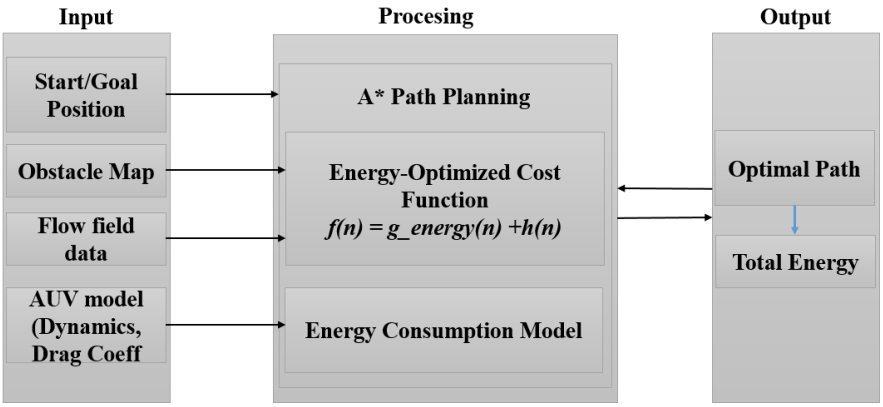

Figure 2. Block diagram of the energy-optimal path planning system for an AUV

The total energy $E_{Total}(\pi)$ for a path $\pi = (s_0, \ldots, s_n)$ combines energy costs across all segments $(s_j \rightarrow s_{j+1})$, as (12):

$$E_{Total}(\pi) = \sum_{j=0}^{n-1} \left[\frac{1}{2} . \rho . C_d \left\| v_{g,j} - v_{c,j} \right\|^3 . \frac{d_j}{\|v_{g,j}\|} + \frac{mg|\Delta h_j|}{\eta} \right] \quad (12)$$

where ρ is water density (kg/m³); C_d is drag coefficient; $v_{g,j}$ is ground velocity vector of the AUV in segment j (m/s); $v_{c,j}$ is ocean current velocity vector in segment *j (m/s)*; d_j is length of segment *j (m)*; m is mass of the AUV (kg); g is gravitational acceleration (9.81 m/s²); Δh_j is depth change in segment j, $\Delta h_j = h(s_{j+1}) - h(s_j)$; η is thruster efficiency ($0 < \eta \leq 1$).

The energy consumed by the propulsion system (propulsion energy) is modeled based on the observation that the propulsion power is approximately proportional to the cube of the relative speed (the AUV's speed relative to the water), as described by (13).

$$E_{prop,i} = k_1 \|v_i\|^3 \Delta t \quad (13)$$

The hydrodynamic drag force (drag loss) acting on the vehicle is modeled as being quadratically dependent on its relative velocity in the water, as described in (14).

$$E_{drag,i} = k_2 \|v_i - v_{\text{current}}(p_i)\|^2 \Delta t \quad (14)$$

To ensure the trajectory ends properly at the desired destination, a terminal cost, or 'goal penalty,' is included in the cost function as shown in (15).

$$\Phi(s_n) = \begin{cases} 0 & if p_n = p_{goal} \\ \infty & otherwise \end{cases} \quad (15)$$

The total energy consumed by the vehicle during the trajectory is calculated by aggregating the energy components discussed earlier, including propulsion energy and other energy changes, as shown in (16).

$$E_{Total}(\pi) = \sum_{i=0}^{n-1} (E_{\text{prop,i}} + E_{\text{drag,i}}) + \Phi(s_n) \quad (16)$$

The optimization problem aims to find the optimal trajectory π* that minimizes total energy consumption subject to all given constraints. This optimal trajectory is presented in (17).

$$\pi^* = argmin\, E_{Total}(\pi) \quad (17)$$

For the A* search implementation, the AUV's workspace is modeled as a graph where nodes are discrete states s_i and edges are transitions between adjacent states. The cost associated with each edge transition is calculated based on the energy expenditure for that segment, including propulsion energy and drag losses $E_{drag,i}$. This value represents the incremental path cost $g(n) = E_{Total}(\pi_{s_0 \rightarrow s_n})$ accumulated by

the algorithm. The overall A* cost function then combines this path cost with a heuristic to efficiently guide the search towards the goal.

The heuristic function *h(n),* presented in (18), is used to estimate the optimal cost from the current state n to the goal, thereby accelerating the search process.

$$h(n) = \frac{k_1 V_{max}^3 + k_2 V_{current}^{-2}}{v_{nom}} . \left\| p_{goal} - p_n \right\| \quad (18)$$

In order to make a transition, the required relative velocity v_{nom} must satisfy $v_{nom} \leq V_{max}$, where V_{max} represents the maximum speed of the AUV.

4. SIMULATION RESULTS

4.1. Simulation setup

The simulation is conducted in an AUV working environment which is a 2D grid map sized 50×50 cells, representing an underwater operational area with resolution corresponding to the grid cell size, and containing static obstacles at specific coordinates and a non-uniform ocean current field modeled as a complex vortex flow. The simulation parameters are listed in Table 1.

Table 1. Simulation parameters

Parameter	Symbol	Value	Unit
Mass of AUV	*m*	*100*	*kg*
Length of AUV	*L*	*1.5*	*m*
Diameter of AUV	*D*	*0.3*	*m*
AUV speed	*v*	*2*	*m/s*
Water density	*ρ*	*1025*	*kg/m^3*
Drag coefficient	*Cd*	*0.15*	
Thruster efficiency	*η*	*0.5*	

4.2. Results

Scenario 1: Simulating the scenario with no obstacles and no current.

Figure 3 illustrates the results of the A* pathfinding algorithm in a simplified scenario, without obstacles or flow. The identified optimal path (blue line) represents the shortest route between the start and goal points, marked by green and red nodes, respectively. The obtained parameters, including a path length of 56.57 meters and a total energy consumption of 2262.74 Joules, demonstrate the algorithm's efficiency in minimizing both distance and energy costs. The results showcase the capability of the A* algorithm in determining effective routes in an unobstructed environment.

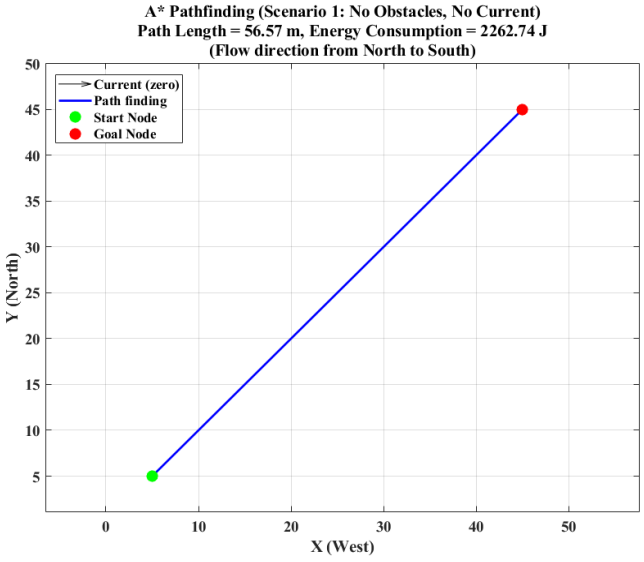

Figure 3. Simulating the scenario with no obstacles and zero flow

Scenario 2: Simulating the scenario with obstacles and no current.

Figure 4 presents the results of applying the A* pathfinding algorithm in a more complex scenario, with the presence of obstacles. The optimized path, depicted by the blue line, is successfully determined to connect the start point (green node) and the goal point (red node) without colliding with the obstacles (red objects). The path parameters, including a length of 58.33 meters and energy consumption of 2333.04 Joules, demonstrate the algorithm's ability to find effective solutions in a more intricate environment compared to the obstacle-free case. This path determination showcases the A* algorithm's capability in path planning within challenging environments.

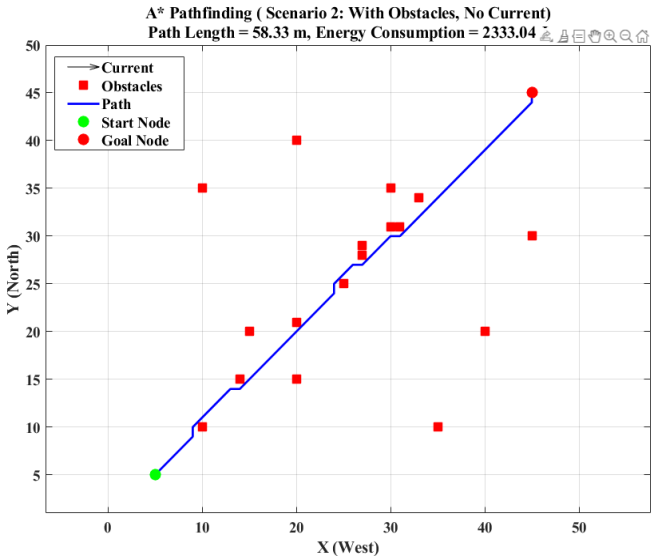

Figure 4. Simulating the scenario with obstacles and no current

Scenario 3: Simulating the scenario complex obstacles present and no current.

Figure 5 demonstrates the A* algorithm's pathfinding within a challenging scenario involving a substantial rectangular obstacle. The algorithm yields an optimized trajectory (blue line), linking the origin and destination points without encountering the obstacle. Key performance indicators, specifically a distance of 74.73 meters and energy expenditure of 2989.12 Joules, quantify the algorithm's performance under these conditions.

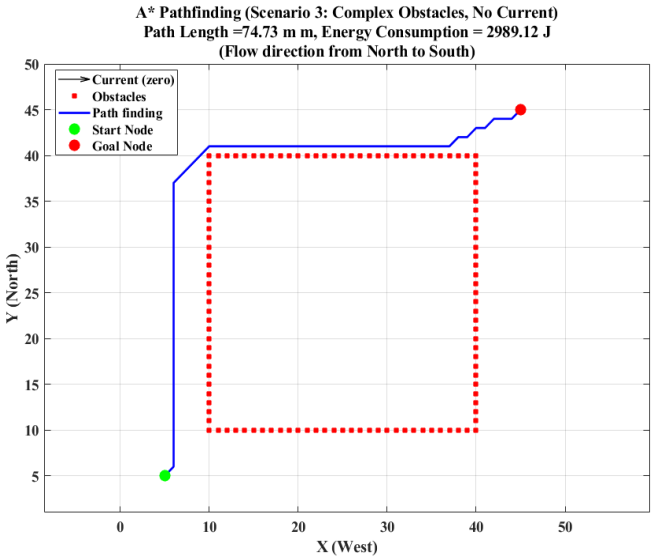

Figure 5. Simulating the scenario with complex obstacles and no current

Scenario 4: Simulating the scenario with current present (weak flow), no obstacles.

Figure 6 illustrates the pathfinding results of the A* algorithm within an environment characterized by a weak flow and without obstacles, comparing both downstream (blue, dashed line) and upstream (red line) paths. While both paths exhibit an equal length of 56.15 meters, the energy costs vary, highlighting the impact of flow on navigation. This difference in energy consumption (2701.07 J for downstream and 2635.17 J for upstream) emphasizes the significance of considering flow dynamics when planning routes in real-world environments, particularly where energy optimization is a primary concern.

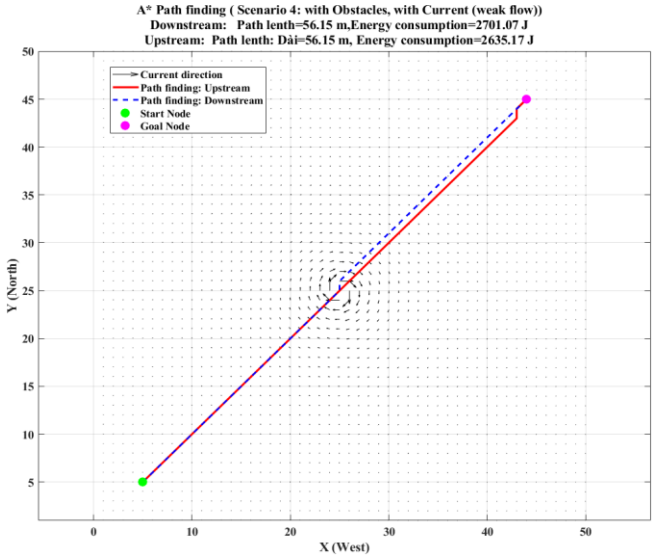

Figure 6. Simulating the scenario with current present (weak flow), no obstacles

Scenario 5: Simulating the scenario with current present (strong flow), no obstacles.

Figure 7 illustrates the pathfinding results of the A* algorithm in an environment with a strong flow but without obstacles. The comparison between the downstream path (blue dashed line) and the upstream path (red line) shows a significant difference in energy costs (47273.84 J versus 57616.09 J) despite the path lengths being nearly identical (56.15 m versus 56.11 m). This emphasizes the substantial impact of strong flow on travel costs.

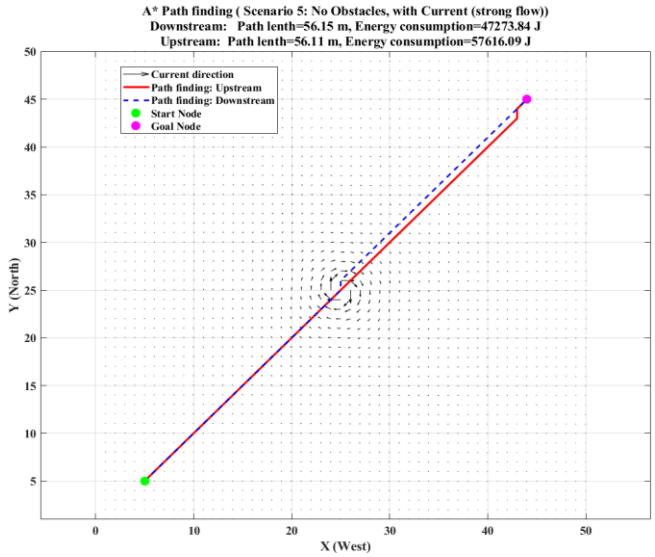

Figure 7. Simulating the scenario with current present (strong flow), no obstacles

Scenario 6: Simulating the scenario with obstacles present, current present (weak flow).

Figure 8 illustrates the A* pathfinding algorithm in an environment with obstacles and a weak flow, comparing the downstream path (blue, dashed line) and the upstream path (red line). Despite the paths having a similar length (56.74 m), the energy consumption differs significantly (2455.72 J downstream and 3997.66 J upstream), reflecting the impact of flow and obstacles on travel energy efficiency.

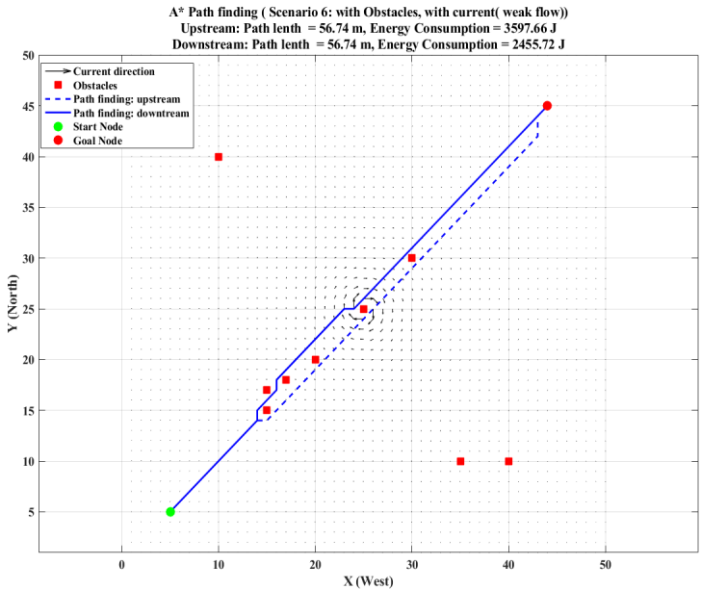

Figure 8. Simulating the scenario with obstacles present, current present (weak flow)

Scenario 7: Simulating the scenario with obstacles present, current present (strong flow).

Figure 9 illustrates the results of the A* pathfinding algorithm in an environment with obstacles and a strong flow. Notably, there is a significant difference in energy costs between the downstream path (solid blue line) at 44517.99 J and the upstream path (dashed blue line) at 82726.39 J, despite the path lengths being nearly identical (57.74 m versus 57.15 m). This highlights the substantial impact of strong flow on travel costs, making upstream travel almost twice as energy-intensive as downstream travel.

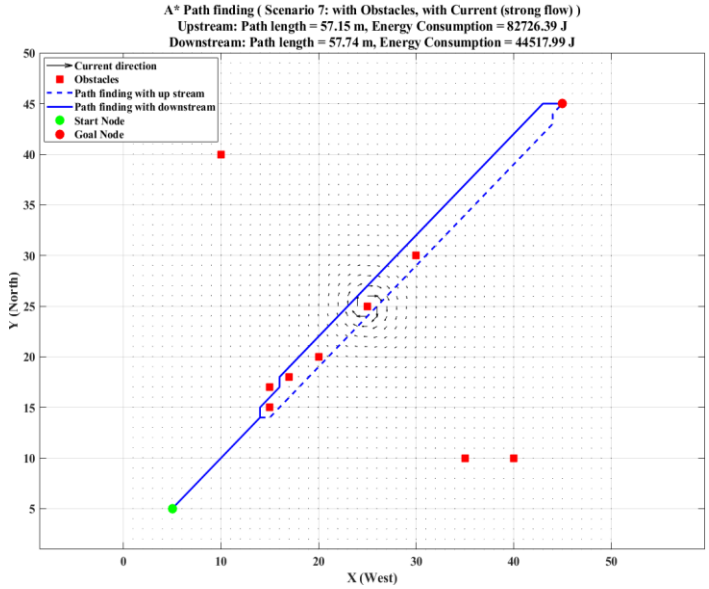

Figure 9. Simulating the scenario with obstacles present, current present (strong flow)

Scenario 8: Simulating the scenario with no possible path exists (goal surrounded by obstacles). This is a test case for algorithm correctness/robustness.

Figure 10 depicts a special case of the A* algorithm where no feasible path exists between the start and goal points due to complete blockage by obstacles. This is indicated by the path length being 0.00 meters and the energy consumption being infinity (Inf J), demonstrating that the algorithm has determined no possible route.

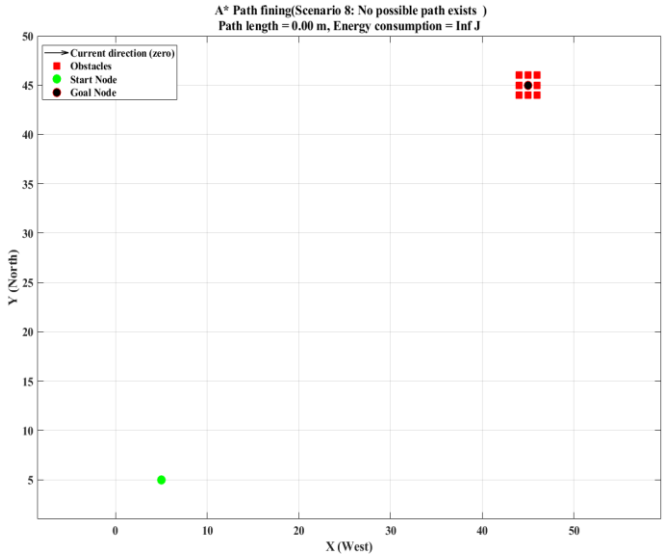

Figure 10. Simulating the scenario with no possible path exists

4.3. Discussion

The simulation results demonstrate the unequivocal superiority of the energy-optimized A* algorithm over the standard geometric A* for minimizing energy consumption in dynamic flow fields. The most significant finding is the substantial energy reduction of up to 50% in scenarios with strong currents (Scenario 7). This improvement directly validates our core contribution: the integration of a physics-based energy model into the path cost calculation.

A comprehensive comparison between the proposed energy-optimized A and the standard A* algorithm, based on key performance indicators, is summarized in Table 2. The results highlight a critical performance trade-off: our algorithm explicitly sacrifices path length optimality to achieve a paramount reduction in energy consumption. Furthermore, a computational trade-off is observed. While the per-node computation cost is higher due to the sophisticated energy model, the overall computational efficiency of the A* framework is maintained, making our method feasible for online path planning.

This quantitative analysis underscores that our method achieves its primary goal of massive energy savings while maintaining the computational practicality necessary for deployment on constrained AUV platforms. Our approach occupies a crucial niche between computational complexity and model fidelity. Compared to methods relying on high-fidelity CFD models [14] or level set equations for optimal control [6] our algorithm is far less computationally intensive, making it suitable for online, reactive path planning on resource-constrained AUV hardware. This directly addresses the limitation of computational tractability raised in [18], [19]. Conversely, compared to other heuristic or learning-based approaches like potential fields [9] or reinforcement learning [17], our method provides deterministic performance and guaranteed optimality within the discrete search space, a significant advantage for safety-critical missions.

The practical implication is that AUVs can achieve significantly longer mission durations and operational ranges in current-prone environments without hardware modifications. This enhances the feasibility of long-term autonomous monitoring and inspection missions. Our method provides a robust, practical, and computationally feasible solution for online energy-optimized path planning.

This study has limitations that point toward valuable future research. First, our model assumes perfect knowledge of the flow field, which is often uncertain in real oceans. Future work will integrate probabilistic current forecasts [24] and robust planning techniques. Second, the kinematic model is simplified; integrating full 6-DOF dynamics would increase fidelity. Third, the computational cost, while

lower than high-fidelity methods, still grows with grid resolution. Investigating more efficient graph representations or hybridized algorithms with evolutionary methods [15], [22] could further enhance scalability. Finally, experimental validation in a water tank with a flow generator and a small AUV is the essential next step to transition this simulation-based research into practical deployment.

Table 2. Comparative analysis of standard A* and energy-optimized A* algorithms

Evaluation Metric	Standard A* (Baseline)	Energy-Optimized A* (Proposed)
Total Energy Consumed (Joules)	Optimizes for path length, ignoring flow effects. - Scenario 5: ~47,273 J (downstream) & ~57,616 J (upstream) - Scenario 7: ~44,518 J (downstream) & ~82,726 J (upstream)	Directly optimized for energy minimization. - Scenario 7: ~50% reduction in energy consumption compared to upstream path. Prioritizes energetically favorable paths.
Path Length (meters)	Optimal: Always finds the shortest geometric path. - Scenario 1: 56.57 m - Scenario 3: 74.73 m	May be sacrificed for energy efficiency. - Can be slightly longer if detouring to leverage currents saves significant energy.
Computation Time (seconds)	Lower (~0.0221 s). Per-node cost is low (*g(n)* is simple Euclidean distance).	Higher(~0.1513 s). Per-node cost is higher due to complex *g_energy(n)* calculations involving *v_rel, drag*, and *flow field lookup*.

5. CONCLUSION

This paper introduces an energy-optimized A* algorithm for AUV path planning within dynamic flow fields. A key contribution is the direct integration of a computationally efficient flow field model and a detailed energy consumption model into the A* search heuristic. The vehicle's motion is described by a 6-DoF (six degrees of freedom) rigid-body kinematic model, while the energy model incorporates critical factors including hydrodynamic drag, the relative velocity between the AUV and the fluid, and the energy costs associated with maneuvering.

The simulation results reveal a clear correlation between environmental complexity and energy consumption in AUV path planning. The algorithm was implemented and validated in a simulated environment with varying flow conditions. Simulation results demonstrate that the proposed energy-optimized A* algorithm achieves a significant reduction in energy consumption (up to 50% in tested scenarios) compared to a standard A* implementation. In simpler scenarios, such as those without obstacles or current, the algorithm efficiently finds the shortest path with minimal energy consumption (Path length = 56.57 meters, energy consumption = 2262.74 Joules in Scenario 1). As complexity increases with the introduction of obstacles, the algorithm successfully navigates around them, with a corresponding increase in path length and energy consumption (Path Length = 74.73 meters, Energy Consumption = 2989.12 Joules in Scenario 3). The presence of ocean currents, particularly strong currents, significantly impacts energy consumption (Energy Consumption = 47273.84 J (Downstream), 57616.09 J (Upstream) in Scenario 5), highlighting the importance of considering flow dynamics in path planning. This work provides a practical solution for energy-aware AUV navigation, contributing to longer mission durations and improved operational efficiency in complex underwater environments.

FUNDING INFORMATION

Authors state no funding involved.

CONFLICT OF INTEREST STATEMENT

Authors state no conflict of interest.

DATA AVAILABILITY

Data availability is not applicable to this paper as no new data were created or analyzed in this study.

REFERENCES

[1] D. Lu, R. Cui, and P. Wang, "Energy efficient path planning of autonomous underwater vehicles for environment modeling," 2014, doi: 10.1109/MFI.2014.6997716.

[2] R. B. Wynn *et al.*, "Autonomous underwater vehicles (AUVs): Their past, present and future contributions to the advancement of marine geoscience," *Marine Geology*, vol. 352, pp. 451–468, 2014, doi: 10.1016/j.margeo.2014.03.012.

[3] M. Panda, B. Das, B. Subudhi, and B. B. Pati, "A comprehensive review of path planning algorithms for autonomous underwater vehicles," *International Journal of Automation and Computing*, vol. 17, no. 3, pp. 321–352, 2020, doi: 10.1007/s11633-019-1204-9.
[4] K. P. Carroll, S. R. McClaran, E. L. Nelson, D. M. Barnett, D. K. Friesen, and G. N. Williams, "AUV path planning: An A∗ approach to path planning with consideration of variable vehicle speeds and multiple, overlapping, time-dependent exclusion zones," in *Proceedings of the 1992 Symposium on Autonomous Underwater Vehicle Technology, AUV 1992*, 1992, pp. 79–84, doi: 10.1109/AUV.1992.225191.
[5] S. Chen, M. Wang, and W. Song, "Hierarchical learning with heuristic guidance for multi-task assignment and distributed planning in interactive scenarios," *IEEE Transactions on Intelligent Vehicles*, vol. 9, no. 11, pp. 6764–6776, 2024, doi: 10.1109/TIV.2024.3369730.
[6] T. Lolla, P. F. J. Lermusiaux, M. P. Ueckermann, and P. J. Haley, "Time-optimal path planning in dynamic flows using level set equations: theory and schemes," *Ocean Dynamics*, vol. 64, no. 10, pp. 1373–1397, 2014, doi: 10.1007/s10236-014-0757-y.
[7] S. Kim and B. An, "Learning heuristic A*: efficient graph search using neural network," in *Proceedings - IEEE International Conference on Robotics and Automation*, 2020, pp. 9542–9547, doi: 10.1109/ICRA40945.2020.9197015.
[8] G. Chen, D. Cheng, W. Chen, X. Yang, and T. Guo, "Path planning for AUVs based on improved APF-AC algorithm," *Computers, Materials and Continua*, vol. 78, no. 3, pp. 3721–3741, 2024, doi: 10.32604/cmc.2024.047325.
[9] J. O. Kim and P. K. Khosla, "Real-time obstacle avoidance using harmonic potential functions," *IEEE Transactions on Robotics and Automation*, vol. 8, no. 3, pp. 338–349, 1992, doi: 10.1109/70.143352.
[10] P. Stankiewicz, Y. T. Tan, and M. Kobilarov, "Adaptive sampling with an autonomous underwater vehicle in static marine environments," *Journal of Field Robotics*, vol. 38, no. 4, pp. 572–597, 2021, doi: 10.1002/rob.22005.
[11] J. Wen, A. Wang, J. Zhu, F. Xia, Z. Peng, and W. Zhang, "Adaptive energy-efficient reinforcement learning for AUV 3D motion planning in complex underwater environments," *Ocean Engineering*, vol. 312, p. 119111, 2024, doi: 10.1016/j.oceaneng.2024.119111.
[12] R. Song, Y. Liu, and R. Bucknall, "A multi-layered fast marching method for unmanned surface vehicle path planning in a time-variant maritime environment," *Ocean Engineering*, vol. 129, pp. 301–317, 2017, doi: 10.1016/j.oceaneng.2016.11.009.
[13] W. Liang *et al.*, "An enhanced ant colony optimization algorithm for global path planning of deep-sea mining vehicles," *Ocean Engineering*, vol. 301, p. 117415, 2024, doi: 10.1016/j.oceaneng.2024.117415.
[14] A. Mokrane, A. C. Braham, and B. Cherki, "UAV path planning based on dynamic programming algorithm on photogrammetric DEMs," in *2020 International Conference on Electrical Engineering, ICEE 2020*, 2020, pp. 1–5, doi: 10.1109/ICEE49691.2020.9249903.
[15] W. Zhang, N. Wang, and W. Wu, "A hybrid path planning algorithm considering AUV dynamic constraints based on improved A* algorithm and APF algorithm," *Ocean Engineering*, vol. 285, p. 115333, 2023, doi: 10.1016/j.oceaneng.2023.115333.
[16] J. C. Kinsey, R. Eustice, and L. L. Whitcomb, "A survey of underwater vehicle navigation: Recent advances and new challenges," in *7th Conference on Manoeuvring and Control of Marine Craft (MCMC'2006)*, 2006, pp. 1–12.
[17] R. S. Sutton and A. G. Barto, *Reinforcement learning: An introduction*. MIT Press, 2018.
[18] Y. Mileyko, G. Reis, M. Chyba, and R. N. Smith, "Energy-efficient control strategies for updating an augmented terrain-based navigation map for autonomous underwater navigation," in *1st Annual IEEE Conference on Control Technology and Applications, CCTA 2017*, 2017, vol. 2017-Janua, pp. 223–228, doi: 10.1109/CCTA.2017.8062467.
[19] V. De Carolis, K. E. Brown, and D. M. Lane, "Runtime energy estimation and route optimization for autonomous underwater vehicles," *IEEE Journal of Oceanic Engineering*, vol. 43, no. 3, pp. 608–619, 2018, doi: 10.1109/JOE.2017.2707261.
[20] R. Mesquita and P. D. Gaspar, "A path planning optimization algorithm based on particle swarm optimization for UAVs for bird monitoring and repelling – simulation results," in *2020 International Conference on Decision Aid Sciences and Application (DASA)*, Nov. 2020, vol. 10, no. 1, pp. 1144–1148, doi: 10.1109/DASA51403.2020.9317271.
[21] R. Terasawa, Y. Ariki, T. Narihira, T. Tsuboi, and K. Nagasaka, "3d-CNN based heuristic guided task-space planner for faster motion planning," in *Proceedings - IEEE International Conference on Robotics and Automation*, 2020, pp. 9548–9554, doi: 10.1109/ICRA40945.2020.9196883.
[22] J. Zhang, X. Ning, and S. Ma, "An improved particle swarm optimization based on age factor for multi-AUV cooperative planning," *Ocean Engineering*, vol. 287, p. 115753, 2023, doi: 10.1016/j.oceaneng.2023.115753.
[23] C. Lu, J. Yang, B. J. Leira, Q. Chen, and S. Wang, "Three-dimensional path planning of deep-sea mining vehicle based on improved particle swarm optimization," *Journal of Marine Science and Engineering*, vol. 11, no. 9, p. 1797, 2023, doi: 10.3390/jmse11091797.
[24] Z. Yan, J. Li, Y. Wu, and G. Zhang, "A real-time path planning algorithm for AUV in unknown underwater environment based on combining PSO and waypoint guidance," *Sensors (Switzerland)*, vol. 19, no. 1, p. 20, 2019, doi: 10.3390/s19010020.

BIOGRAPHIES OF AUTHORS

Do Khac Tiep received his BS from Electrical and Electronics Department of Vietnam Maritime University, Haiphong, Vietnam in 2009. He received MS degree of Vietnam Maritime University in 2012. From 2009 to 2015, he was a teacher at Viet Nam Maritime University. He received his Ph.D degree in the Department of Control Engineering and Robotics, Mokpo National University, South Korea, in 2019. He is currently a lecturer at the Department of Electric and Electronics Engineering of Vietnam Maritime University. His research interests are control of automation control theory, robot control and power plant on ship. He can be contacted at email: dokhactiep@vimaru.edu.vn.

Nguyen Van Tien received his B.S and M.S degrees in Electrical and Electronics Department and Automation from the Vietnam Maritime University in 2009 and 2012, respectively. He received his Ph.D. degree in electric and control engineering from the Mokpo National Maritime University, Korea, in 2018. He is currently a lecturer at the Department of electric and electronics engineering of Vietnam Maritime University. His research interests are control of industrial machines, Robot control, LabVIEW software, and Recycling energy. He can be contacted at email: nguyenvantien@vimaru.edu.vn.

Cao Duc Thanh received the B.S. degree in industrial automation engineering from Vietnam Maritime University, Hai Phong, Vietnam, in 2018 and the M.S. degree in control and automation engineering from Hanoi University of Science and Technology, Hanoi, Vietnam, in 2021. He is currently pursuing the Ph.D. degree in control and automation engineering at Hanoi University of Science and Technology, Hanoi, Vietnam. He is currently a lecturer at the Department of electric and electronics engineering of Vietnam Maritime University. His research includes the development of motion planning control, anti-sloshing control and industrial robot control. He can be contacted at: caoducthanh@vimaru.edu.vn.